A computational study of the optical response of strongly coupled metal nanoparticle chains

ARTICLE *in* OPTICS COMMUNICATIONS · FEBRUARY 2008

Impact Factor: 1.45 · DOI: 10.1016/j.optcom.2007.10.019 · Source: arXiv

2 AUTHORS:

Kin Hung Fung
The Hong Kong Polytechnic University
69 PUBLICATIONS **768** CITATIONS
SEE PROFILE

Che Ting Chan
The Hong Kong University of Science and T…
298 PUBLICATIONS **9,649** CITATIONS
SEE PROFILE

Available online at www.sciencedirect.com
ScienceDirect
Optics Communications 281 (2008) 855–864
OPTICS COMMUNICATIONS
www.elsevier.com/locate/optcom

A computational study of the optical response of strongly coupled metal nanoparticle chains

Kin Hung Fung *, C.T. Chan

Department of Physics, The Hong Kong University of Science and Technology, Clear Water Bay, Hong Kong, China

Received 1 June 2007; received in revised form 3 October 2007; accepted 11 October 2007

Abstract

We study the optical response of strongly coupled metal nanoparticle chains using rigorous multiple scattering calculations. The collective resonant frequency of silver nanosphere chains and the coupling between chains are considered. The coupling between silver nanoparticle chains are understood by the transmission and reflection calculations of 2D periodic arrays of nanospheres. The results are in agreement with recent experiments. The splitting of plasmon resonance modes for different polarizations of the incident light are explored. Our results show that the transverse mode resonant wavelength is very sensitive to the inter-chain distance. Results on the effect of disorder are also presented.

PACS: 78.67.Bf; 73.22.Lp; 71.45.Gm; 78.70.−g

Keywords: Plasmonic resonance; Collective resonance; Metal nanoparticle; Optical response

1. Introduction

The excitation of surface plasmon on metal nanoparticles has attracted the attention of many researchers because of many plausible applications such as surface-enhanced Raman scattering [1,2], subwavelength waveguides [3], biosensors [4] and non-linear optics [5]. Recently, many techniques are developed for the fabrication of metal nanoparticles (MNPs) in form of clusters and ordered structures [6,7]. MNP chains are of particular interest because they may serve as building blocks for plasmonic optical waveguides in nanoscale [3,8,9].

Previous research has focused on optical properties of MNPs with diameters from tens to hundreds of nanometers. For MNPs with diameters $d \sim 10$ nm, there were studies that focused on nanoparticle dimers [10–13], small clusters [14–16] and 2D arrays [17–19]. For chains [20–22] of MNPs of such a size range, experimentally and theoretically obtained optical extinction spectra were compared by Sweatlock et al. recently [23] using finite integration techniques [24] to study the length dependence of the plasmon resonance frequency of a chain of Ag nanospheres (fixing $d = 10$ nm). In that experiment, the authors studied the optical response of a collection of strongly coupled parallel MNP chains. The theoretical calculations, usually, consider a single chain, ignoring the inter-chain couplings. Here, we present the results obtained by the multiple scattering theory (MST), which is highly precise numerically for spherical objects. We consider the size dependence, chain-to-chain coupling, as well as order and disorder issues. In addition, we employ simple models to understand the rigorously calculated results.

This paper is organized as follows. In Section 2, we describe the methods and the system parameters. Section 3 gives the calculated results. We first understand the extinction spectra of MNP chains using simple models. Then, we discuss the phenomena due to the coupling of MNP chains and the effect of order and disorder in a chain, which is followed by the discussion and conclusion in Section 4.

* Corresponding author.
E-mail address: polar@ust.hk (K.H. Fung).

0030-4018/$ - see front matter © 2007 Elsevier B.V. All rights reserved.
doi:10.1016/j.optcom.2007.10.019

2. Methods and parameters

We consider Ag nanospheres (diameter d) embedded in a glass matrix of refractive index $n = 1.61$. The dielectric function of Ag spheres has the form, [10,25,26]

$$\varepsilon(\omega) = \varepsilon_a - \frac{(\varepsilon_b - \varepsilon_a)\omega_p^2}{\omega(\omega + i\gamma)}, \quad (1)$$

where $\varepsilon_a = 5.45$, $\varepsilon_b = 6.18$ and $\omega_p = 1.72 \times 10^{16}$ rad/s. This dielectric function is a fitting of the literature values [27]. The collision frequency γ for d around 10 nm has the form [28]

$$\gamma = \frac{v_F}{l} + \frac{v_F}{R}, \quad (2)$$

where $v_F = 1.38 \times 10^6$ m/s is the Fermi velocity, $l = 52$ nm is the electron mean free path at room temperature and $R = d/2$. Although there is no consensus among different authors about the proportionality between R and d, [29] the relation $R = d/2$ is supposedly safe to use [10]. The prototypical systems that we considered are very similar to those in the literature such as Refs. [17,23], but the adjusted form of the collision frequency represents a more realistic situation.

We use MST to calculate the optical response of Ag nanosphere chains. The MST formalism can be found in details elsewhere [30,31]. It basically employs vector spherical harmonics to expand the EM fields, and the solution of the Maxwell's equations can be made as accurate as we please by increasing the angular momentum (L) cut-off in our expansion. For single chain of a finite number of spheres, we use the MST formulation for a finite number of particles [30,32]. For two-dimensional (2D) arrays, we use the layer MST formulation for periodic systems [31]. Unless it is specified, the truncation angular momentum L in the multipole expansions is 10. We note that all numerical results in this paper are calculated using local theory only. Non-locality issues are discussed in Section 4.

3. Results

3.1. Single metal nanoparticle chain

To facilitate the understanding of the plasmonic resonances of MNP multi-chains (Section 3.3), we first consider a chain of Ag nanospheres of finite length with diameter $d = 10$ nm and surface-to-surface spacing $\sigma = 3$ nm (center-to-center spacing = 13 nm) embedded in the glass matrix. We set an incident electromagnetic plane wave that propagates in the direction perpendicular to the chain axis. The extinction cross sections, calculated by MST, of the chain with the number of spheres $N = 1, 2, 3, \ldots, 10$ are shown in Fig. 1. When there is one single sphere, an extinction peak is found at the photon energy of about 3.0 eV. This corresponds to the Fröhlich mode of the small sphere when the dielectric constant ε of the sphere matches the condition [29]

$$\varepsilon = -2\varepsilon_h, \quad (3)$$

where ε_h is the dielectric constant of the surrounding medium (glass in this case). If we do a multipole expansion of the field, the extinction peak corresponds to the "$L = 1$"

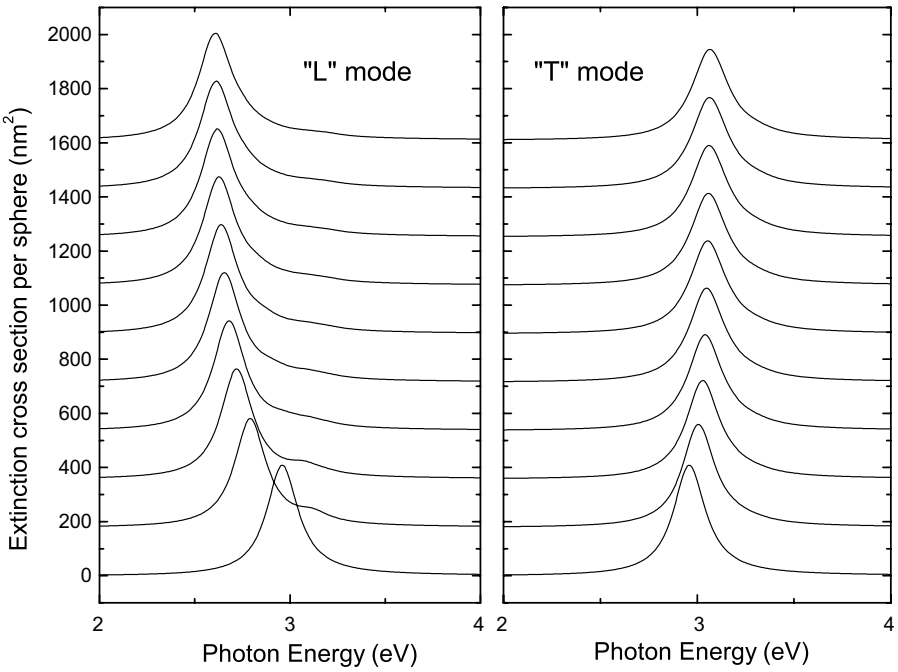

Fig. 1. Extinction spectra of a chain of Ag nanospheres with $d = 10$ nm and $\sigma = 3$ nm. Results are obtained by MST with $L = 10$. Incident wavevector is perpendicular to the chain axis. The curves from bottom to top correspond to different number of spheres from 1 to 10. The left panel corresponds to "L" mode excitation (electric field parallel to the chain axis). The right panel corresponds to "T" mode excitation (electric field perpendicular to the chain axis).

mode (or dipole mode) resonance. The result shows that higher order multipoles contribute very little to the extinction cross sections for such small spheres (see Fig. 2). When $N = 2$, the extinction peak for the dimer splits into two for different light polarizations. We call the excitation mode for incident light polarized parallel (perpendicular) to the chain axis the "L" ("T") mode excitation. We see that the "L" mode extinction peak shifts towards a lower frequency (or photon energy) while the "T" mode peak shifts towards a higher frequency. Similar results are obtained theoretically in Refs. [10,23] and experimentally in Refs. [20,23], and also for different kinds of metal nanoparticles [6,22,33]. In addition to the shift of the resonance frequency, a careful examination of the result also reveal higher multipole ($L > 1$) contributions at about 3.1 eV, but the extinction curves are basically dominated by the dipole ($L = 1$) term. If we compare our MST results with the finite integration calculations in Ref. [23], the obtained resonant frequencies are very similar but the extinction spectra obtained by MST calculations do not exhibit the artifact modes due to the faceted corners of the rendered spheres in Ref. [23].

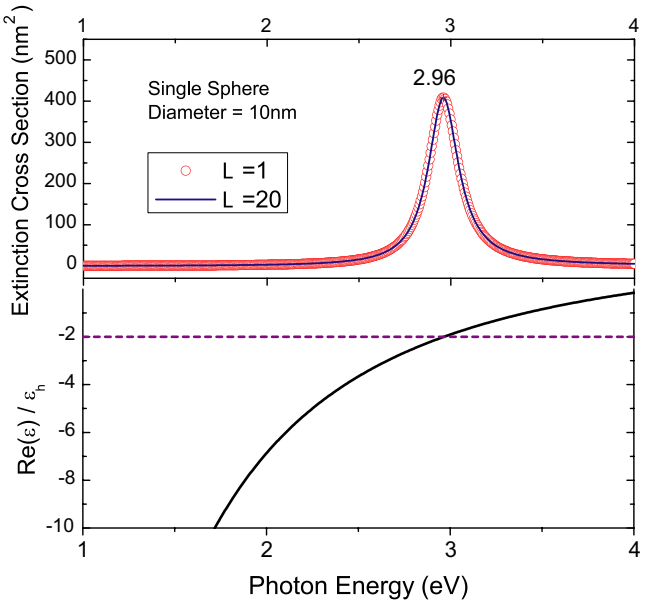

Fig. 2. Extinction spectra of a single Ag nanosphere of diameter 10 nm. Results for different truncation angular momenta ($L = 1$ and 20) in MST calculations are compared. Solid line shown in the lower panel is the real part of the dielectric function divided by that of the host medium.

Here, let us present an intuitive explanation of the shifts of the extinction peak. Fig. 3 shows a schematic induced charge distribution of a finite nanoparticle chain for both the "L" and "T" mode. For a single sphere, the natural oscillation (with frequency ω_0) of the induced charges is provided by a self-induced restoring force that is due to the non-uniform surface charge distribution on its own surface, and the natural frequency is related to the surface plasmon frequency of a spherical surface. When the incident light has a frequency close to ω_0 (i.e., at resonance), the extinction is significantly enhanced. It is obvious that when the spheres are sufficiently close together (but not in contact), the restoring force magnitude on the plasma in each sphere can be significantly affected by others. For "L" mode oscillation, the charge distribution on the nearest spheres attracts the charge displaced by the external field and reduces the restoring force, thus reduces the natural oscillation frequency ω_0. In contrary, the charge distribution in the "T" mode oscillation increases ω_0. Fig. 1 also shows that the peaks shift in the same way as we further increase N to form a chain. For a short chain, a further increase in the number of spheres will further reduce (enhance) the restoring force for "L" ("T") mode (see Fig. 3). A plot of the peak frequency versus N for a finite chain with $\sigma = 2$, 4, and 6 nm is shown in Fig. 4a.

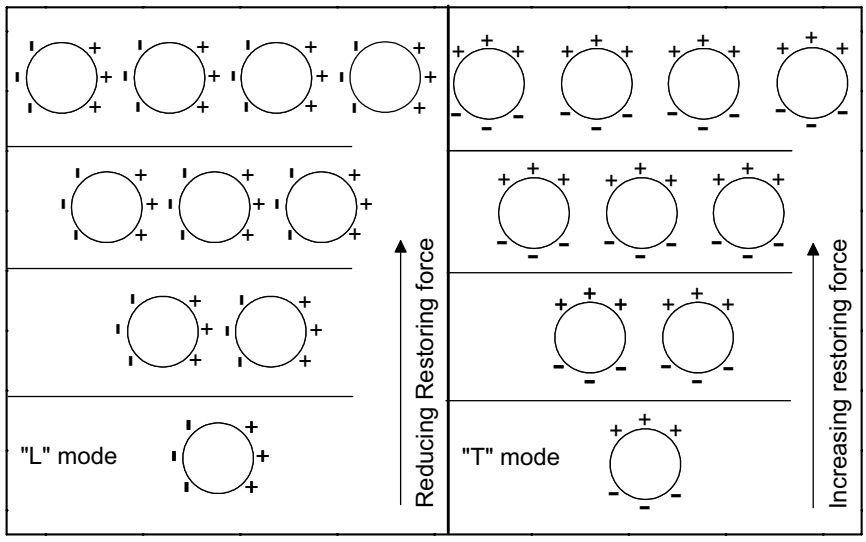

Fig. 3. Schematic diagram of the induced charge distributions on the Ag spheres at long wavelength mode. The left (right) panel corresponds to "L" ("T") mode excitation.

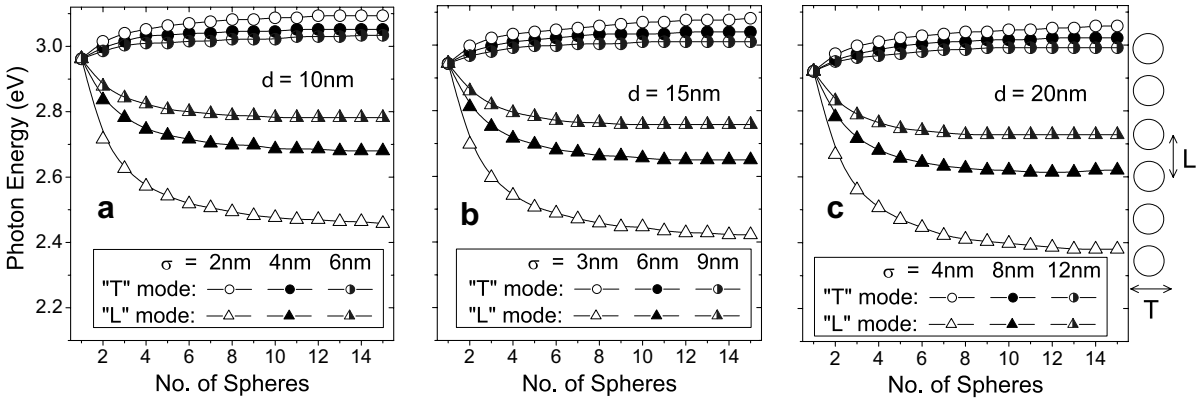

Fig. 4. Extinction peak frequency versus length of Ag nanosphere chain for different separation σ and polarizations. Results are obtained by MST with $L = 10$. Incident wavevector is perpendicular to the chain axis: (a) $d = 10$ nm; (b) $d = 15$ nm; (c) $d = 20$ nm.

This figure shows that, when N is large, the "L" mode and "T" mode approach to an asymptotic value of about 2.5 and 3.09 eV for $\sigma = 2$ nm, 2.7 and 3.05 eV for $\sigma = 4$ nm, 2.8 and 3.03 eV for $\sigma = 6$ nm. Let us call these frequencies the long chain resonance frequencies. As we can see later, these values correspond to the long wavelength collective plasmon modes of an infinite long chain of metal spheres. We found that the frequency shift of "L" mode is larger than that of "T" mode. Therefore, the "L" mode coupling is stronger than "T" mode coupling for such configuration.

Corresponding figures for $d = 15$ and 20 nm (with the same scaling ratio in σ) are shown in Fig. 4b and c. A summary of the long chain resonance frequencies obtained here is shown in Table 1. These results are qualitatively the same, which means the phenomena are not sensitive to the size of particles. The estimated long chain resonant frequencies will help us understand the coupling of chains in Section 3.3.

3.2. Dipolar model

The results presented in Figs. 1, 2 and 4 are (essentially exact) numerical solution of the Maxwell's equations. Here, we employ a simple model to give a semi-quantitative analysis. Since the full multiple scattering results, in Section 3.1, show that the optical response is mainly dominated by the dipole ($L = 1$) terms (see Fig. 1 and 2), it should be a good approximation to employ a dipolar model (we note that the dipolar model is only employed in this subsection for understanding the phenomena only). The dispersion relations of a long and infinite chain of MNPs using dipolar model has been considered previously [34–39]. We now focus on the quasi-eigen plasmonic modes of a short chain and its relation to the long chain limit. When there is no external field, the dipole moment of the sphere m induced by other dipoles is [40]

$$\mathbf{p}_m = \alpha(\omega) \sum_{m' \neq m} \frac{(1-\beta_{m'm})[3(\hat{\mathbf{r}}_{m'm} \cdot \mathbf{p}_{m'})\hat{\mathbf{r}}_{m'm} - \mathbf{p}_{m'}] + \beta_{m'm}^2[(\hat{\mathbf{r}}_{m'm} \cdot \mathbf{p}_{m'})\hat{\mathbf{r}}_{m'm} - \mathbf{p}_{m'}]}{r_{m'm}^3} \times e^{\beta_{m'm}}, \tag{4}$$

where $\alpha(\omega)$ is the polarizability of the spheres, $\beta_{m'm} = \frac{in\omega r_{m'm}}{c}$, n is the refractive index of the host medium (with $\mu_h = 1$), $\mathbf{r}_{m'm}$ is the position vector of sphere m' measured from sphere m, and c is the velocity of light in vacuum. For an arbitrary arrangement of non-touching spheres, Eq. (4) can be written as the general form

$$\sum_{m'} \sum_{\sigma'} M_{m'\sigma'}^{m\sigma} p_{m'\sigma'} = 0, \tag{5}$$

where $p_{m'\sigma'}$ is the σ'th component of the dipole moment of sphere m' in Cartesian coordinates and $M_{m'\sigma'}^{m\sigma}$ is a matrix at a given angular frequency ω and arrangement of the spheres. In the case we discuss in this paper, the nanospheres are arranged as a chain so that Eq. (5) reduces to

Table 1
Comparison among the long chain plasmon resonance photon energies obtained in Fig. 4 for finite chain and Fig. 7 for 2D array

d (nm)	σ (nm)	Finite chain		2D array	
		L (eV)	T (eV)	L (eV)	T (eV)
10	2	2.46	3.09	2.47	3.10
10	4	2.68	3.05	2.69	3.07
10	6	2.78	3.03	2.79	3.04
15	3	2.42	3.08	2.45	3.10
15	6	2.65	3.04	2.67	3.06
15	9	2.76	3.01	2.77	3.02
20	4	2.38	3.06	2.42	3.09
20	8	2.62	3.02	2.64	3.05
20	12	2.73	2.99	2.74	3.01

$$\sum_{m'} M^m_{m'} p_{m'} = 0, \tag{6}$$

where

$$M^m_{m'} = \begin{cases} \frac{1}{\alpha(\omega)} & \text{for } m = m' \\ [(1 - \beta_{m'm} + \beta^2_{m'm}) - g(3 - 3\beta_{m'm} + \beta^2_{m'm})] \frac{e^{\beta_{m'm}}}{r^3_{m'm}} & \text{for } m \neq m' \end{cases} \tag{7}$$

In Eq. (7), $g = 1$ for the "L" mode and $g = 0$ for the "T" mode. In the quasistatic limit, we use $\alpha(\omega) = \frac{\varepsilon(\omega)-\varepsilon_h}{\varepsilon(\omega)+2\varepsilon_h}\left(\frac{d}{2}\right)^3$. Here, we do not use the radiation reaction correction $\left(\frac{1}{\alpha(\omega)} \to \frac{1}{\alpha(\omega)} - i\frac{2\omega^3}{3c^3}\right)$ because we are dealing with complex $\varepsilon(\omega)$ [41–43]. In matrix representation, we seek for the non-trivial solutions, $\mathbf{p}$, by solving the equation

$$\det[\mathbf{M}(\omega)] = 0. \tag{8}$$

The roots of Eq. (8) (eigen-frequencies of the system), ω_n, are in general complex [36,39,44] with $\mathrm{Im}(\omega_n) < 0$. However, it may be possible to observe a resonant response at certain excitation frequency close to $\mathrm{Re}(\omega_n)$ as long as $\mathrm{Im}(\omega_n)$ is small. In our case, $\mathrm{Im}(\omega_n) \approx -0.1$ eV such that $|\mathrm{Im}(\omega_n)|/|\mathrm{Re}(\omega_n)| < 4\%$ for all ω_n that we found.

For the 1D finite chain of Ag nanoparticles, we have compared the extinction peak frequency with $\mathrm{Re}(\omega_n)$. Results for $N = 1$–7 are shown in Fig. 5a and b. When there are N spheres, we get N quasi-eigen frequencies satisfying Eq. (6). As the number of spheres increases and reaches the limit $N \to \infty$, the chain becomes periodic and the quasi-eigen frequencies form a band. The Brillouin zone boundary and zone center mode frequencies (for $N \to \infty$) are also shown in the figures. For the "L" mode, the band has a positive group velocity and the zone center ($k = 0$) mode has a lower frequency than the zone boundary mode. However, the opposite is true for the "T" mode band that can have a negative group velocity [36,35,39]. We see that the extinction peak calculated by fully-fledged MST agrees quite well with the resonance of the quasi-eigen mode at the lowest (highest) frequency for "L" ("T") mode of the dipolar model. This can be explained by the following arguments. The incident wave is a plane wave with wavevector perpendicular to the chain axis (i.e., the external incident field on all spheres are in-phase). The quasi-eigen mode with the largest number of in-phase

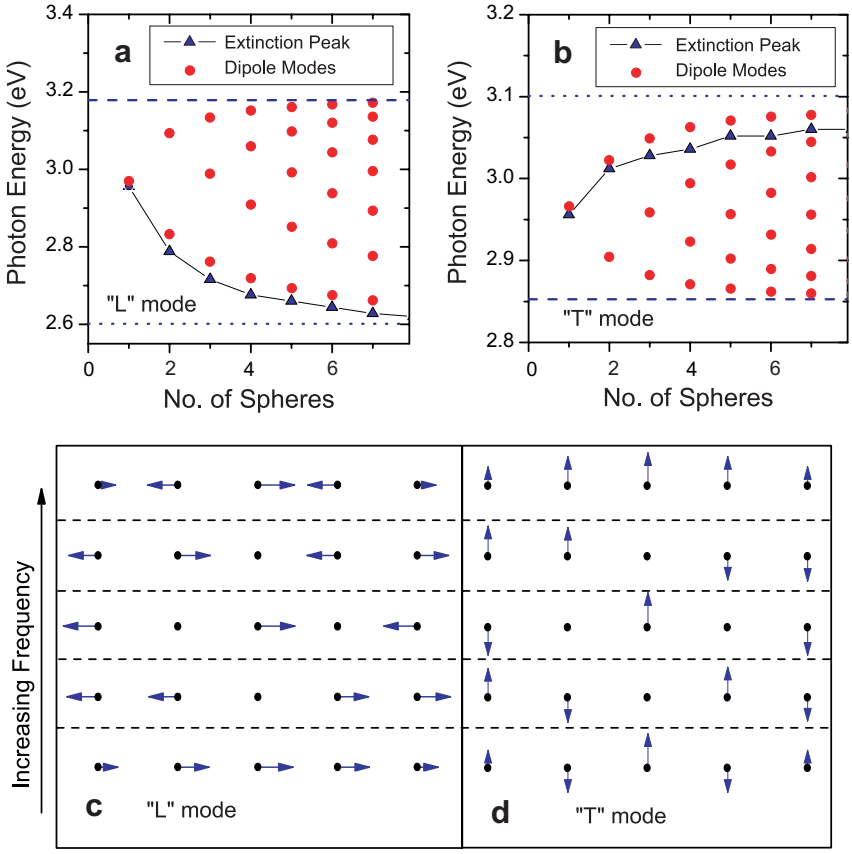

Fig. 5. Comparison between the resonance modes (as a function of the chain length) calculated by the MST and dipolar model. Only the real part of the eigen-frequencies are shown: (a) and (b) show the quasi-eigenmode frequencies calculated by solving Eq. (8) with $d = 10$ nm and $\sigma = 3$ nm together with the extinction peak frequencies (given by MST) for "L" and "T" mode, respectively. The dashed and dotted lines are, respectively, the Brillouin zone boundary and zone center mode frequencies (for $N \to \infty$) calculated by the dipolar model; (c) and (d) show the instantaneous dipole vectors of a dipole chain with number of particles $N = 5$ at different eigenmodes.

dipoles thus contributes most resonant response because the symmetry of the mode is closest to that of the external incident field. Therefore, for "L" ("T") mode, the lowest (highest) frequency eigen mode is the one that can be excited at normal incidence (see Fig. 5c and d).

3.3. Coupling of MNP chains

We now look at the optical response of Ag nanospheres in a two-dimensional array. The purpose of doing so is to study the coupling between nanoparticle chains. In the experiment of Ref. [20], the sample contains numerous coupled nanoparticle chains that are almost aligned in the same direction. However, the chain-to-chain coupling are ignored in the corresponding numerical calculations. [20] Although the lengths of nanoparticle chains in the experiment may be short, it is worth to have a quantitative study of infinitely long chains for comparison.

In this MST calculation, the sphere radii are the same as those for the nanoparticle chains we discussed. Let **a** and **b** denote the two primitive lattice vectors constructing an infinite 2D periodic array. We note that the chain-to-chain coupling is still not well understood, although many papers have considered 2D array of MNPs (e.g., Ref. [17]). For the purpose to study the inter-chain coupling, we choose the case $\mathbf{a}\perp\mathbf{b}$. When $b \gg a$, the system will act like an array of independent infinitely long nanoparticle chains. When $b \approx a$, the system can be considered as a collection of coupled nanoparticle chains, which corresponds to the experiment of Ref. [20]. Calculated transmission, reflection and absorption spectra at normal incidence for $b = a$, $1.2a$, and $2a$ are shown in Fig. 6. For $b \neq a$, the figure shows only the "$\mathbf{E}\|\mathbf{b}$" mode. For simplicity, we will also call the "$\mathbf{E}\|\mathbf{b}$" the "T" mode because it corresponds to the "T" mode of single chain when $b \gg a$. The same notation applies to "$\mathbf{E}\|\mathbf{a}$" mode and "L" mode. We see that the dominant reflection peak, absorption peak and the transmission dip are located at the same frequency, which corresponds to the plasmon resonant frequency. Again, the dipole response dominates in this case. There are only some

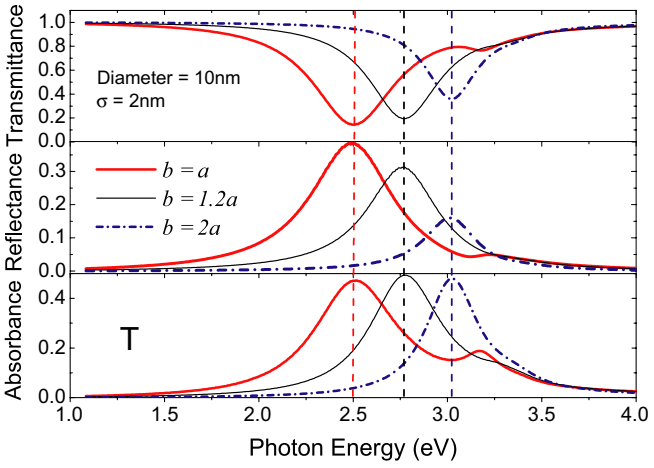

Fig. 6. Transmission, reflection and absorption spectra of Ag nanospheres arranged in 2D infinite rectangular lattice with $a = 12$ nm and $d = 10$ nm at normal incidence. Results are obtained by MST with $L = 10$. For $b \neq a$, only the "T" modes are shown.

small features at 3.2 eV that are due to higher order resonances. In this case, the consequence of the coupling between nanoparticle chains is a shift in the plasmon resonant frequency. By varying the ratio between **a** and **b**, we can study such frequency shift due to the coupling between nanoparticle chains in greater details. We vary the magnitude of **b** and repeat the calculations. A plot of the resonant frequencies versus b/a (fixing a and varying b) for two different light polarizations is shown in Fig. 7a. Let us define $\sigma = a - d$. The figure shows that as **b** increases, the "L" mode ($\mathbf{E}\|\mathbf{a}$) and "T" mode ($\mathbf{E}\|\mathbf{b}$) resonant peak shifts from 2.51 to the asymptotic values of 2.47 and 3.10 eV for $\sigma = 2$ nm, from 2.71 to 2.69 and 3.07 eV for $\sigma = 4$ nm, from 2.80 to 2.79 and 3.04 eV for $\sigma = 6$ nm. Corresponding figures for $d = 15$ and 20 nm (with the same scaling ratio in σ) are shown in Fig. 7b and c. All these limits obtained from the graphs agree with the long chain resonance frequencies obtained for the single finite chain that we have discussed in Section 3.1. This consistency is expected because the limit $b \gg a$ for 2D case and the limit

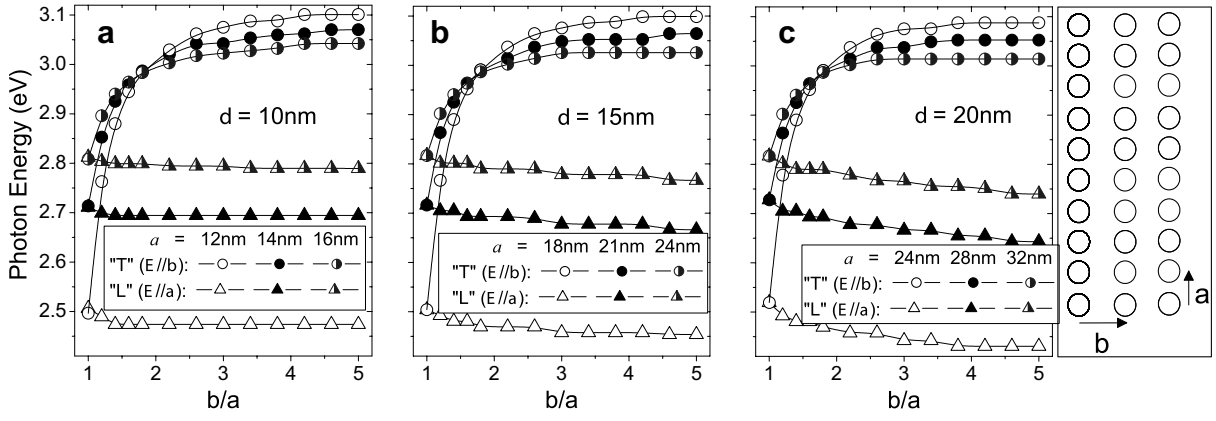

Fig. 7. Resonance frequencies obtained from the reflection curves of a 2D infinite rectangular array of Ag nanospheres at normal incidence. Results are obtained by MST with $L = 10$. (a) $d = 10$ nm; (b) $d = 15$ nm; (c) $d = 20$ nm.

$N \to \infty$ for "single chain" case are both representing non-interacting nanoparticle chain(s). In addition, the results in Fig. 7b and c show again that the salient features are not sensitive to the particle size.

Here, we see that the splitting of resonant frequency is significant enough to be observed as long as b/a is greater than about 2. This is an important criteria of observing the chain properties in the experiment of Ref. [20]. For $b < 2a$, the chains are strongly coupled. Our results show that the "T" mode resonance frequency is very sensitive to a small change, Δb, in the inter-chain distance. In terms of the change in resonant wavelength, $\Delta\lambda$, we found that $\Delta\lambda/\Delta b$ can be as high as 20. In contrary, the "L" mode resonance frequency is insensitive to Δb. It is also observed that when the chains are close to each other ($b \approx a$), i.e., the spheres are arranged in square lattice, the resonant peaks are still lower than the single sphere resonance ($\sim$2.96 eV). In this special case, assigning the "L" mode and "T" mode is in fact not suitable because both "L" mode and "T" mode couplings among nanospheres are present simultaneously. The situation then can be considered as a competition between "L" and "T" mode. From the fact that "L" ("T") mode tends to reduce (increase) the resonance frequency, we see that "L" mode coupling wins over "T" mode coupling. This is also consistent with Section 3.1 that "T" mode coupling is much weaker than "L" mode coupling. Therefore, it suggests that the extinction peak will be lower in general when the nanospheres are close but not in contact ($\sigma \sim 3$ nm). Indeed, it was found that this is true for many other 2D structures [17], but this will not be discussed in details in this paper because we now focus on the chain properties. Another interesting feature is that the curves for "T" mode in Fig. 7 cross the point at $b/a \sim 1.8$ with photon energy 2.98 eV. This frequency is very close to the single sphere resonant frequency. This is where the competition between "L" and "T" mode coupling ends in a draw.

3.4. The effect of periodicity

The Ag nanoparticle chains discussed in the previous sections are arranged such that the center-to-center distances of adjacent spheres in a chain are the same. One may be interested in the question that whether this structural order can produce an extra structural resonance other than the resonance of individual spheres. However, this does not occur in our case. For the parameters that we used previously, the possible extra resonance should be at a very high frequency such that the wavelength of the incident light is comparable to the sphere-to-sphere distances. However, such a high frequency is out of the range of interest of the present article. Searching for such effect to compare with previous results, we increase the center-to-center distances to 400 nm.

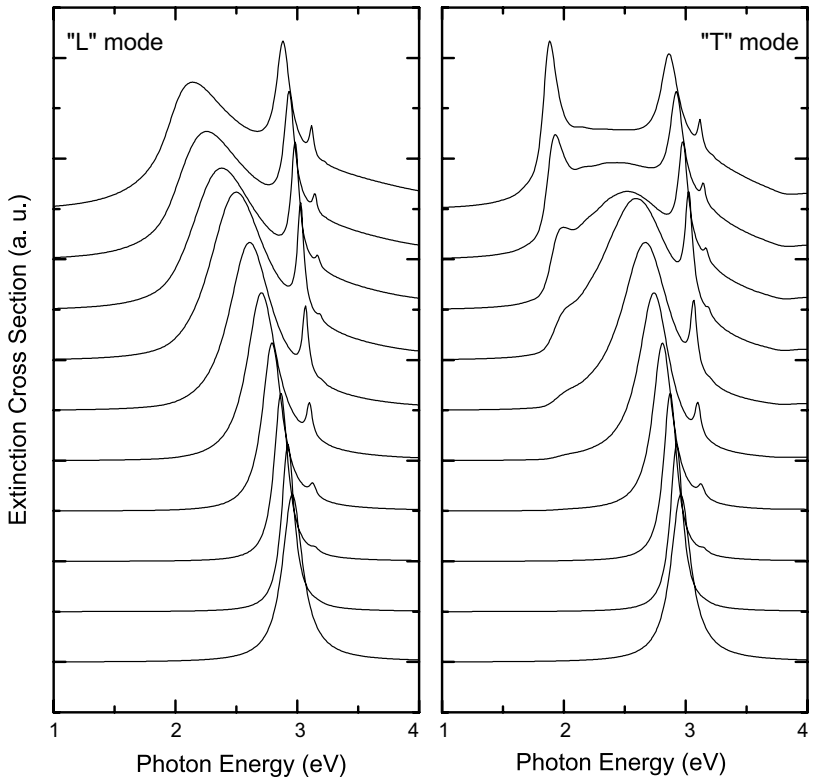

Fig. 8. Extinction spectra of Ag nanospheres chain consisting of 10 spheres with center-to-center separation $a = 400$ nm. Incident wavevector is perpendicular to the chain axis. The curves from bottom to top correspond to different diameters from 10 to 100 nm in 10 nm increment. Each curve is normalized in different scale so that the resonance frequencies can be easily compared.

The extinction spectrum for a 10-sphere chain with d increases from 10 to 100 nm in steps of 10 nm is shown in Fig. 8. We note that the dielectric functions of spheres with different diameters follow Eqs. (1) and (2). When $d = 10$ nm, the extinction has no difference from that of a single sphere (except the overall amplitude of the profile). As we increase the sphere diameter, we see a gradual red shift of the "$L = 1$" (Fröhlich mode) resonance peak. This is a general feature of the Fröhlich resonance [29]. Higher multipole ($L > 1$) resonances also appear near 3 eV when $d \geqslant 40$ nm, and can be traced to the higher order resonances of a single sphere. Apart from these known effects, we can see an additional feature that is due to the structural order. When we increase the sphere diameters so that $d > 80$ nm, an extra sharp peak appears at about 1.88 eV for "T" mode excitation but not for the "L" mode. Such photon energy corresponds to a wavelength of 410 nm (close to the sphere-to-sphere distance) in the host material. This feature [45–48] is due to the constructive interference of the scattered waves from the nanospheres and cannot be seen from the extinction spectra of a single sphere. For convenience, we call this peak a Bragg resonant peak.

Here, we have two points to note. The first one is why "small" Ag nanospheres cannot make a Bragg peak. The reason is that the extinction spectra of "small" Ag nanospheres are dominated by absorption while that of large Ag nanospheres are dominated by scattering [6]. The Bragg peak that we are searching is a consequence of strong scattering. Therefore, this Bragg peak does not appear for d around 10 nm. Secondly, the strength of the far field scattered wave of a radiating dipole decays as r^{-2} in the polar direction while it decays as r^{-1} in a direction perpendicular to the polar direction. This explains why only "T" mode but not "L" mode excitation can make the Bragg peak.

Using dipolar approximations, some authors shows that the Bragg peak can be extremely sharp [46,47]. However, the sharpness of such peak requires an exact periodic arrangement of nanospheres. To understand how such peak is sensitive to disorder, we consider a 20-sphere linear array. In this example, we have an ensemble of 25 randomly generated configurations with the diameter of each sphere $d = 100$ nm and the center-to-center separation given by the expression $a = 400\text{ nm} + r_1 \times 40\text{ nm}$, where r_1 is a random number generated uniformly from -1 to 1. The particular extinction spectrum of each randomly generated nanosphere array are shown in Fig. 9. In the same figure, the averaged extinction spectra (of the 25 configurations) is also compared with that of the regular array (with $r_1 = 0$). It is clear that the resonant peaks at higher frequencies (>2.5 eV) do not depend on disorder. The curves shown in the figure are basically the same in this frequency range (2.25 to 3.5 eV). It is because these peaks are the higher order resonances of individual sphere. In contrary, the Bragg peak is significantly affected by the orderliness of the chain (see Fig. 9 (upper panel)). Although the Bragg peak for an ordered chain can be much sharper than

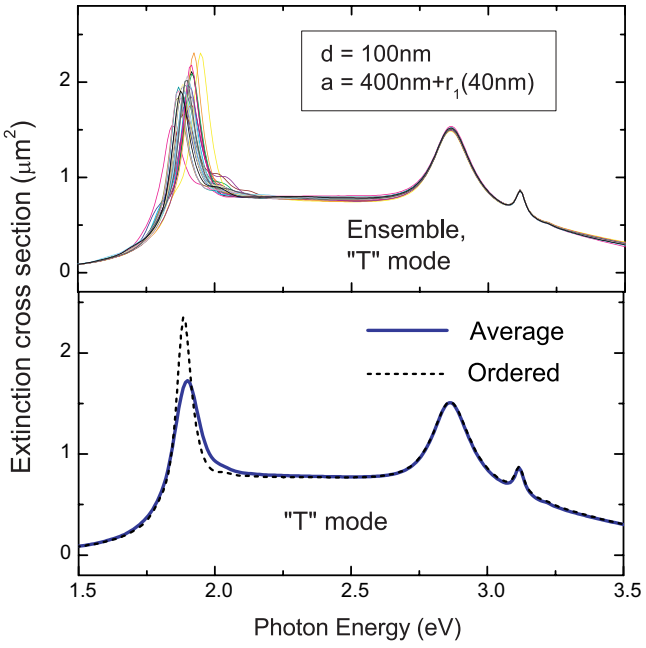

Fig. 9. Extinction spectra of Ag nanosphere chain consisting of 20 nanospheres for "T" mode. The upper panel shows 25 particular spectra for $d = 100$ nm and $a = 400\text{ nm} + r_1 \times 40$ nm, where r_1 is a random number generated uniformly from -1 to 1. The lower panel shows the average spectrum and the spectrum corresponding to $r_1 = 0$.

the higher order plasmon resonance peaks, this is only true when we have perfect periodicity. Disorder will smooth out the sharp Bragg features (see Fig. 9 (lower panel)). We note that the Bragg peak frequency is inversely proportional to the adjacent sphere-to-sphere distance ($\omega_B \sim 1/a$). For a small change in distance δa, we have $\omega_B + \delta\omega \sim 1/(a + \delta a)$, from which we see that a finite positive δa gives a smaller red shift $|\delta\omega|$ while a negative δa of the same magnitude gives a larger blue shift $|\delta\omega|$. Therefore, in the case that r_1 being generated uniformly from -1 to 1, the Bragg peak of the averaged curve has a blue shift.

3.5. Disordered finite chain

In the previous section, we showed that the sharpness of the Bragg resonance peak is sensitive to random dislocations of the nanospheres. However, such resonance contributes very little to the extinction spectra for the values of σ and d used in Section 3.1. It thus suggests that the qualitative feature of extinction spectra should remain even if there is some randomness in the surface-to-surface distances, σ, of adjacent spheres. To see the robustness of the plasmon resonant features that we obtained, we have also studied an ensemble of 25 randomly generated configurations for each polarization. There is a chain of 10 nanospheres in each configuration. Diameter of each sphere and the surface-to-surface distance are given by, respectively, the expressions $d = 10\text{ nm} + r_1 \times 2\text{ nm}$ and $\sigma = 3\text{ nm} + r_2 \times 1\text{ nm}$, where r_1 and r_2 are random numbers generated uniformly from -1 to 1. Note again that the

dielectric functions of spheres with different diameters are different according to Eq. (1) and (2). The particular and averaged extinction spectra are shown in Fig. 10. It is clear that the difference of the averaged curve from the ordered chain is very little. The profile as long as the center of peak and the peak height are almost not affected by disorder. An observable difference shown in Fig. 10b for "L" mode is a red shift. This can be understood by referring back to Fig. 7. The results in Fig. 7 show that, for a fixed chain length, the red shift in the peak frequency with σ reducing from 4 to 2 nm is larger than the blue shift with σ increasing from 4 to 6 nm. It suggests that reducing σ has a larger effect than increasing σ when the amounts of changes in σ are the same. This explains the red shift in Fig. 10b. Using the similar arguments, there should also be a blue shift in Fig. 10d for "T" mode, but the shift is too small to be observed from the figure. Nevertheless, the little dependence on disorder shows the reason why the resonant features are still experimentally observable as in Ref. [20].

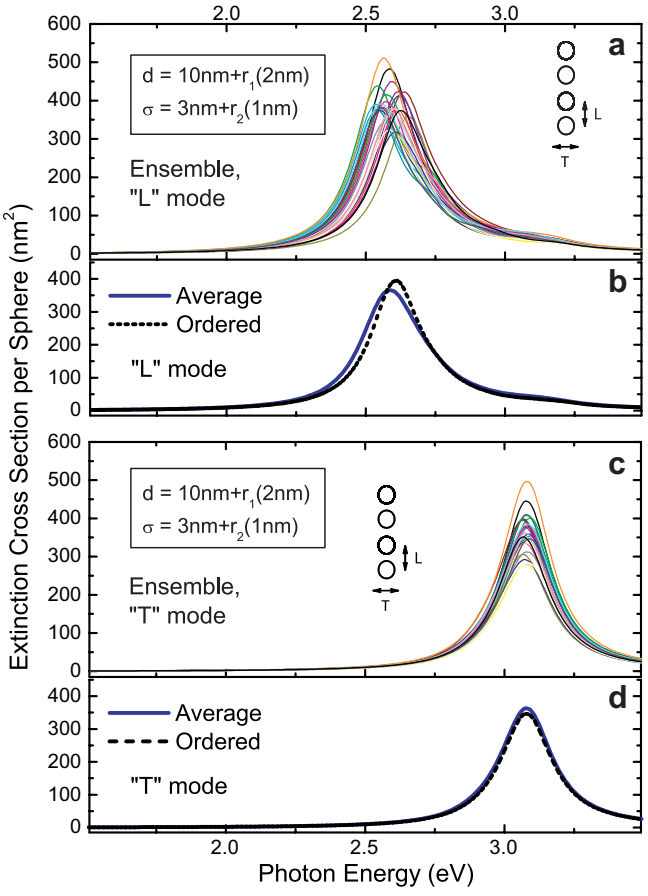

Fig. 10. Extinction spectra of Ag nanosphere chain consisting of 10 nanospheres. Panels (a) and (c) show 25 particular spectra for "L" and "T" excitations with $d = 10\text{ nm} + r_1 \times 2\text{ nm}$ and $\sigma = 3\text{ nm} + r_2 \times 1\text{ nm}$, where r_1 and r_2 are random numbers generated uniformly from -1 to 1. Panels (b) and (d) show the averaged spectrum and the spectrum corresponding to all r_1 and r_2 equal zero for "L" and "T" excitations, respectively.

4. Discussion and conclusion

Using MST, we studied the optical response of strongly coupled Ag nanoparticle chains. We showed that the "T" mode resonant wavelength is very sensitive to the inter-chain distance. The ratio of change in resonance wavelength to the inter-chain distance can be as high as $\Delta\lambda/\Delta b \approx 20$. We also showed that the nanoparticle chain properties are already observable when the chain-to-chain spacing is greater than twice of the particle-to-particle spacing in a chain. This result and the disorder issues discussed in Sections 3.4 and 3.5 explain why the splitting phenomena of plasmon resonant band can be observed experimentally.

The numerical results presented in this paper are the full multiple scattering calculations which are based on the Mie theory. We note that we have not yet added any non-local correction in our calculations. Non-local effect due to small particle size (typically for $d < 10$ nm) will give corrections to the the results obtained with local theories [49]. We expect there is a typical blue shift in the resonant frequencies in the range of frequency that we are interested. For aggregated particles with very small surface-to-surface distance, the non-local effect may also be significant, and those should be topics of future studies. However, Pack et al. showed that such surface non-local effect in a pair of silver spheres of particle diameter $d = 10$ nm is negligible when the surface-to-surface spacing $\sigma > 0.4$ nm. [13] In our present work, $\sigma > 2$ nm in glass (corresponding to $\sigma > 3.2$ nm in air) for all the cases we considered.

Acknowledgements

This work was supported by the Central Allocation Grant from the Hong Kong RGC through HKUST3/06C. Computation resources were supported by the Shun Hing Education and Charity Fund. We also thank Prof. Z. F. Lin and Dr. Jack Ng for useful discussions.

References

[1] M. Moscovits, Rev. Mod. Phys. 57 (1985) 783.
[2] G. Bachelier, A. Mlayah, Phys. Rev. B 69 (2004) 205408.
[3] S.A. Maier, P.G. Kik, H.A. Atwater, S. Meltzer, E. Harel, B.E. Koel, A.A.G. Requicha, Nat. Mater. 2 (2003) 229.
[4] A.J. Haes, R.P.V. Duyne, J. Am. Chem. Soc. 124 (2002) 10596.
[5] See, e.g.: M. Danckwerts, L. Novotny, Phys. Rev. Lett. 98 (2007) 026104.
[6] U. Kreibig, M. Vollmer, Optical Properties of Metal Clusters, Springer, Berlin, 1995.
[7] D.L. Feldheim, C.A. FossJr. (Eds.), Metal nanoparticles: synthesis, Characterization and Applications, Marcel Dekker, New York, 2002.
[8] M. Quinten, A. Leitner, J.R. Krenn, F.R. Aussenegg, Opt. Lett. 23 (1998) 1331.
[9] R. Quidant, C. Girard, J.C. Weeber, A. Dereux, Phys. Rev. B 69 (2004) 085407.
[10] J.J. Xiao, J.P. Huang, K.W. Yu, Phys. Rev. B 71 (2005) 045404.
[11] P. Nordlander, C. Oubre, E. Prodan, K. Li, M.I. Stockman, Nano Lett. 4 (2004) 899.
[12] B. Khlebtsov, A. Melnikov, V. Zharov, N. Khlebtsov, Nanotechnology 17 (2006) 1437.

[13] A. Pack, M. Hietschold, R. Wannemacher, Opt. Commun. 194 (2001) 277.
[14] A. Taleb, V. Russier, A. Courty, M.P. Pileni, Phys. Rev. B 59 (1999) 13350.
[15] S.K. Lim, K.J. Chung, C.K. Kim, D.W. Shin, Y.H. Kim, C.S. Yoon, J. Appl. Phys. 98 (2005) 084309.
[16] S.E. Sburlan, L.A. Blanco, M. Nieto-Vesperinas, Phys. Rev. B 73 (2006) 035403.
[17] L.L. Zhao, K.L. Kelly, G.C. Schatz, J. Phys. Chem. B 107 (2003) 7343.
[18] A.F. Koenderink, J.V. Hernndez, F. Robicheaux, L.D. Noordam, A. Polman, Nano Lett. 7 (2007) 745.
[19] A.I. Rahachou, I.V. Zozoulenko, J. Opt. A 9 (2007) 265.
[20] J.J. Penninkhof, A. Polman, L.A. Sweatlock, S.A. Maier, H.A. Atwater, A.M. Vredenberg, B.J. Kooi, Appl. Phys. Lett. 83 (2003) 4137.
[21] Y. Yang, S. Matsubara, M. Nogami, J.L. Shi, W.M. Huang, Nanotechnology 17 (2006) 2821.
[22] Y.J. Kang, K.J. Erickson, T.A. Taton, J. Am. Chem. Soc. 127 (2005) 13800.
[23] L.A. Sweatlock, S.A. Maier, H.A. Atwater, J.J. Penninkhof, A. Polman, Phys. Rev. B 71 (2005) 235408.
[24] Maxwell's Equations by Finite Integration Algorithm, Gesellschaft fur Computer-Simulationstechnik, Darmstadt, Germany, 2000.
[25] P.G. Kik, S.A. Maier, H.A. Atwater, Phys. Rev. B 69 (2004) 045418.
[26] M. Moskovits, I. Srnová-loufová, B. Vlková, J. Chem. Phys. 116 (2002) 10435.
[27] P.B. Johnson, R.W. Christy, Phys. Rev. B 6 (1972) 4370.
[28] D.P. Peters, C. Strohhöfer, M.L. Brongersma, J. van der Elsken, A. Polman, Nucl. Instrum. Meth. B 168 (2000) 237.
[29] C.F. Bohren, D.R. Huffman, Absorption and Scattering of Light by Small Particles, Wiley, New York, 1983.
[30] Y.L. Xu, Appl. Opt. 34 (1995) 4573.
[31] N. Stefanou, V. Yannopapas, A. Modinos, Comput. Phys. Commun. 113 (1998) 49.
[32] J. Ng, Z.F. Lin, C.T. Chan, P. Sheng, Phys. Rev. B 72 (2005) 085130.
[33] S.A. Maier, M.L. Brongersma, P.G. Kik, H.A. Atwater, Phys. Rev. B 65 (2002) 193408.
[34] D.S. Citrin, Nano Lett. 4 (2004) 1561.
[35] C.R. Simovski, A.J. Viitanen, S.A. Tretyakov, Phys. Rev. E 72 (2005) 066606.
[36] W.H. Weber, G.W. Ford, Phys. Rev. B 70 (2004) 125429.
[37] A. Alù, N. Engheta, Phys. Rev. B 74 (2006) 205436.
[38] A.F. Koenderink, A. Polman, Phys. Rev. B 74 (2006) 033402.
[39] K.H. Fung, C.T. Chan, Opt. Lett. 32 (2007) 973.
[40] J.D. Jackson, Classical Electrodynamics, third ed., Wiley, New York, 1998.
[41] Quasistatic polarizability with a radiation correction is appropriate when the dielectric constant ε is real. This correction term is purely imaginary and is in the order of x^3 ($x =$ size parameter). However, when ε is complex, there is an additional correction term, which has an imaginary part in the order of x^2. Therefore, using only the radiation correction (x^3), but ignoring the absorption correction (x^2), is inappropriate when absorption is considered. Indeed, the most appropriate form of $\alpha(\omega)$ is the electric dipole coefficient a_1 in the Mie theory. In our case, $x \ll 1$ and the spheres are not too close so that using the quasistatic form of $\alpha(\omega)$ is already enough for a good understanding of the more rigorously calculated results given by MST. More detailed discussions about the dipole approximations can be found in Refs. [42] and [43].
[42] C.E. Dungey, C.F. Bohren, J. Opt. Soc. Am. A 8 (1991) 81.
[43] B.T. Draine, P.J. Flatau, J. Opt. Soc. Am. A 11 (1994) 1491.
[44] The complex root-searching method is not an efficient method for solving the problem, but it is commonly used in the literatures. A more efficient and accurate eigen-decomposition method can be found in Ref. [39].
[45] S. Zou, N. Janel, G.C. Schatz, J. Chem. Phys. 120 (2004) 10871.
[46] S. Zou, G.C. Schatz, J. Chem. Phys. 121 (2004) 12606.
[47] V.A. Markel, J. Phys. B 38 (2005) L115.
[48] S. Zou, G.C. Schatz, Nanotechnology 17 (2006) 2813.
[49] P. Halevi (Ed.), Spatial Dispersion in Solids and Plasmas, Elsevier, North-Holland, 1992.